

SAGE: Agentic Framework for Interpretable and Clinically Translatable Computational Pathology Biomarker Discovery

Sahar Almahfouz Nasser*¹ Juan Francisco Pesantez Borja*² Jincheng Liu*² Tanvir Hasan*³
 Zenghan Wang*² Suman Ghosh*² Sandeep Manandhar*¹ Shikhar Shiromani² Twisha Shah²
 Naoto Tokuyama¹ Anant Madabhushi¹

Abstract

Despite significant progress in computational pathology, many AI models remain black-box and difficult to interpret, posing a major barrier to clinical adoption due to limited transparency and explainability. This has motivated continued interest in engineered image-based biomarkers, which offer greater interpretability but are often proposed based on anecdotal evidence or fragmented prior literature rather than systematic biological validation.

We introduce SAGE (Structured Agentic system for hypothesis Generation and Evaluation), an agentic AI system designed to identify interpretable, engineered pathology biomarkers by grounding them in biological evidence. SAGE integrates literature-anchored reasoning with multi-modal data analysis to correlate image-derived features with molecular biomarkers, such as gene expression, and clinically relevant outcomes.

By coordinating specialized agents for biological contextualization and empirical hypothesis validation, SAGE prioritizes transparent, biologically supported biomarkers and advances the clinical translation of computational pathology.

1. Introduction

Recent advances in large language models (LLMs) (Luo et al., 2022), (Singhal et al., 2023), and (Remy et al., 2022) have enabled agentic systems capable of synthesizing scientific literature, generating hypotheses, and coordinating analytical workflows. Within this landscape, two prevailing paradigms have emerged.

¹Department of Biomedical Engineering, Emory University, Atlanta, GA, USA ²Georgia Institute of Technology, Atlanta, GA, USA ³University of Arkansas at Little Rock, Little Rock, AR, USA. Correspondence to: Anant Madabhushi <anantm@emory.edu>.

Preprint. February 3, 2026.

The first paradigm, largely driven by the machine learning community, emphasizes autonomous hypothesis generation and novelty discovery. Systems in this category, such as SciAgents (Ghafarollahi & Buehler, 2024) and AutoGPT-Sci (Park et al., 2023), excel at creative exploration but typically deprioritize biological grounding, interpretability, and clinical feasibility. As a result, the hypotheses they generate, while often novel, are difficult to contextualize within established biomedical knowledge or translate into clinically actionable insights.

The second paradigm, primarily originating from the biomedical research communities such as NOVA (Vaidya et al., 2025) and WSI-Agents (Lyu et al., 2025), focuses on clinically motivated biomarker discovery using vision-language models, static pipelines, or expert-guided tools. Although aligned with diagnostic and prognostic objectives, these approaches often rely on black-box models or expert priors and lack explicit biological explanations linking computational features to molecular mechanisms. Consequently, many such biomarkers face barriers to independent validation and clinical adoption.

This dichotomy—novelty without interpretability or clinical utility on one side, and clinical intent without novelty or biological grounding on the other—represents a central limitation of current computational pathology research. Addressing this limitation requires systems that are explicitly designed to discover biomarkers that are biologically grounded, interpretable, and feasible for clinical validation.

To this end, we introduce **SAGE**, a structured agentic system that unifies biomarker discovery, biological interpretation, and empirical validation within a single end-to-end pipeline. Unlike prior agentic frameworks that prioritize generation alone, SAGE is purpose-built to bridge computational pathology features with molecular biomarkers and clinical outcomes through literature-grounded reasoning and multi-modal data analysis.

SAGE coordinates specialized agents with distinct scientific roles. An Ontologist agent explores non-obvious biological relationships from medical literature; a Scientist agent

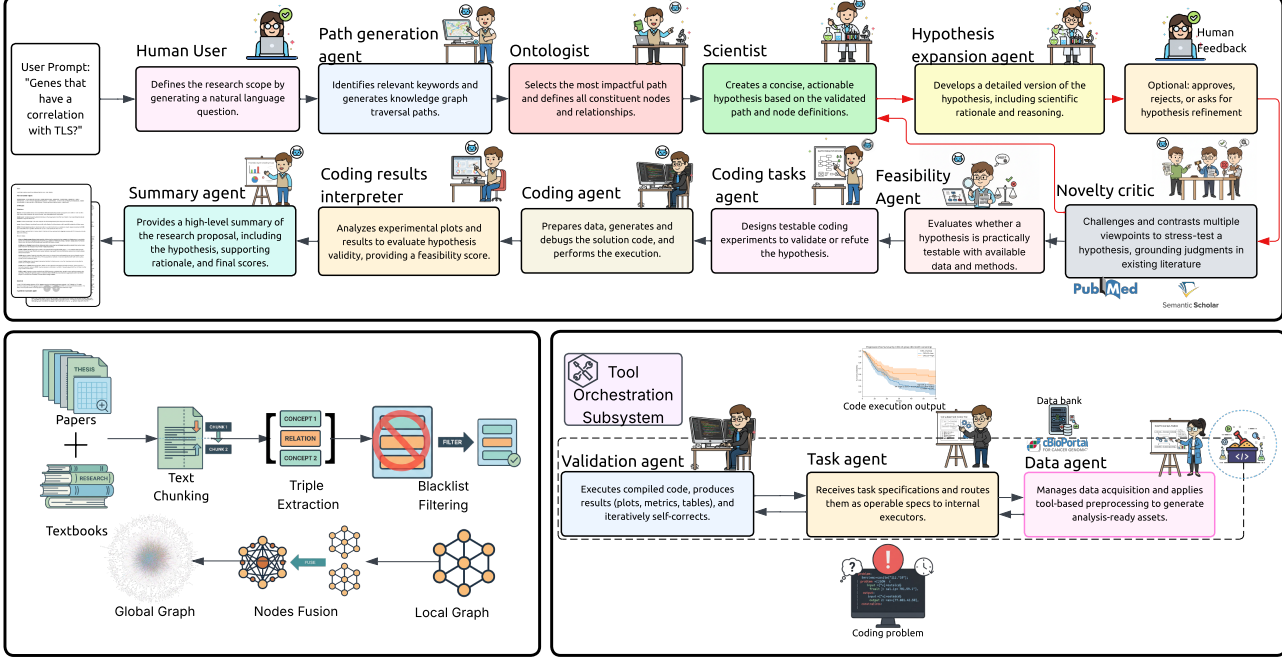


Figure 1. Overview of the SAGE framework for computational pathology. The pipeline comprises three stages: (1) *Knowledge graph construction and reasoning* (bottom left), integrating pathology-aware biomedical entities to support structured biological reasoning; (2) *Hypothesis generation and refinement* (top), where coordinated agents produce interpretable hypotheses linking image-derived pathology features with molecular and clinical endpoints; and (3) *Validation and summarization* (bottom right), which executes statistical analyses and generates clinically interpretable summaries. Figure 5 in the supplementary material details the pathology-aware tool orchestration subsystem.

formulates candidate hypotheses; a Senior Scientist agent grounds these hypotheses by linking imaging-derived features with molecular and clinical biomarkers; a Clinical Feasibility agent evaluates interpretability and validation readiness; a Debate-based Critic assesses scientific novelty; and a Coding agent executes hypothesis validation on patient cohorts, with a Summary agent consolidating results.

By structuring agent responsibilities around biological grounding, interpretability, feasibility, and validation, SAGE prioritizes explainable and clinically meaningful discoveries while suppressing spurious associations.

We summarize our contributions as follows:

- Biologically Grounded Agentic Design:** An agentic system explicitly structured to discover and interpret pathology-derived biomarkers, demonstrated using bladder cancer as a motivating use case.
- Multi-Path Ontological Reasoning:** An ontological exploration strategy that uncovers diverse, biologically plausible connections across imaging, molecular, and clinical domains.
- Debate-Based Novelty Assessment:** A structured multi-agent mechanism for transparent and reliable

scientific novelty evaluation.

- End-to-End Validation Pipeline:** Automated translation of hypotheses into executable analyses for empirical validation on multi-modal computational pathology datasets.

2. Related Work

Recent agentic and language-model-driven systems in computational pathology have primarily focused on interactive analysis, task execution, and tool orchestration over whole slide images (WSIs). Approaches such as PathChat (Lu et al., 2024), NOVA (Vaidya et al., 2025), and WSI-Agents (Lyu et al., 2025) enable conversational querying, automated pipeline execution, and collaborative slide interpretation through multi-agent coordination. While effective for streamlining analysis and supporting user-driven interpretation, these systems are fundamentally designed around *task completion* rather than *scientific discovery*.

More broadly, agentic scientific discovery with large language models can be decomposed into three components: (i) representation of prior knowledge, (ii) hypothesis generation, and (iii) empirical validation. Existing work typically addresses these components in isolation or emphasizes

hypothesis generation without enforcing biological coherence or validation readiness. As a result, many generated hypotheses remain speculative, weakly interpretable, or disconnected from clinically actionable endpoints.

In contrast, SAGE bridges this gap by integrating literature grounding, multi-modal biological interpretation, clinical feasibility assessment, and empirical hypothesis validation within a single end-to-end agentic system designed for clinical adoption.

2.1. Representation of Prior Knowledge

Knowledge graphs (KGs) provide the backbone for automated reasoning by encoding biomedical and molecular relationships in structured form. Early integrative biomedical graphs such as Hetionet (Himmelstein et al., 2017) and BioKG (Zhang et al., 2025) demonstrated that heterogeneous, expert-curated KGs could support systematic drug-repurposing and disease-mechanism discovery. Recent graph-learning work focuses on scalability and semantic precision: Tree-KG (Niu et al., 2025) introduces hierarchical expansion strategies for efficient KG growth; GraphMERT (Belova et al., 2025) distills relational knowledge from text using transformer encoders; and GEPA (Agrawal et al., 2025) proposes graph-guided prompt evolution to improve reasoning fidelity. These approaches motivate expert-guided yet automatically expandable knowledge representations, which SAGE adopts to ground hypothesis generation.

2.2. Hypothesis Generation

Automated hypothesis generation has been explored through LLM prompting, symbolic induction, and multi-agent collaboration. Zhou et al. (Zhou et al., 2024) showed that few-shot prompting and iterative feedback can yield coherent scientific hypotheses. Frameworks such as SciAgents (Ghafarollahi & Buehler, 2024) and AgentFlow (Li et al., 2025) employ coordinated LLM teams for structured reasoning and planning, while POPPER (Hillerstrom & Burghouts, 2024) demonstrates complementary symbolic logic-programming for interpretable induction. GEPA (Agrawal et al., 2025) and Tree-of-Thoughts (Yao et al., 2023) explore reflective and search-based prompting to improve reasoning depth. Despite these advances, most systems lack a flexible hypothesis validation layer. SAGE advances hypothesis-generation frameworks by unifying multi-path ontological reasoning, novelty debate, clinical feasibility assessment, and empirical validation in a task-aware, efficient pipeline.

2.3. Empirical Hypothesis Validation

Despite progress in agentic reasoning, empirical hypothesis validation remains a key bottleneck in AI-driven scientific workflows. Systems such as ResearchCodeAgent (Gandhi

et al., 2025) integrate LLMs with predefined analysis scripts, but their fixed execution logic limits adaptability to newly generated hypotheses.

By contrast, SAGE adopts a validation-first design in which each generated hypothesis is automatically translated into executable code, closing the reasoning-to-validation loop and enabling quantitative assessment without manual intervention.

3. Method

3.1. Knowledge Graph Construction

SAGE constructs a domain-specific biomedical knowledge graph (KG) from scientific literature using a multi-stage pipeline inspired by Buehler et al. (Buehler, 2024). The goal is to transform unstructured text into a machine-interpretable representation of entities, relations, and supporting evidence that can ground downstream reasoning and hypothesis generation. As summarized in Figure 1, the pipeline consists of literature filtering, triple extraction, graph construction, and quality assessment. Additional implementation details are provided in the supplementary material A.

Literature Processing and Triple Extraction: We begin by automatically screening candidate papers to ensure corpus relevance and quality (Ouzzani et al., 2016). Expert-curated keyword sets spanning computational pathology and bladder cancer-specific concepts are used to score papers based on semantic relevance, SapBERT similarity (Reimers & Gurevych, 2019), and publication venue. Approximately 40% of initially retrieved papers are filtered as irrelevant.

Text is extracted from retained PDFs, normalized, and segmented into overlapping chunks of approximately 1,500 tokens. Each chunk is processed by an LLM (GPT-4o-mini) to extract biomedical triples of the form $(h, t_h, r_{text}, r_{norm}, t, t_t, c, e)$, where h and t denote head and tail entities, t_h and t_t their ontology types, r_{text} the surface relation, r_{norm} its normalized form, $c \in [0, 1]$ a confidence score, and e the supporting evidence span. Triples with $c \geq 0.5$ are retained, and relations are normalized via ontology-aware rule-based mapping (Peng et al., 2017; Zhang et al., 2018).

Graph Construction and Fusion: We synthesize a unified global knowledge graph \mathcal{G}_{global} via a two-stage fusion strategy. Local directed graphs $G_d = (V_d, E_d)$ are first constructed from each document d , with edges weighted by extraction confidence. To resolve cross-document entity redundancy, we perform node fusion using BGE-Large embeddings (Xiao et al., 2023) with a cosine similarity threshold of $\tau = 0.9$, merging redundant edges via weight summation. Finally, we prune disconnected components to ensure topological coherence, serializing the resulting graph in GraphML format (Brandes et al., 2001) for downstream

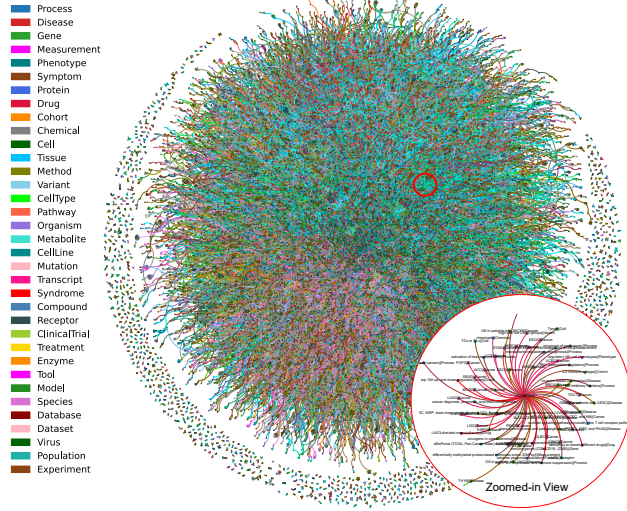


Figure 2. Biomedical Knowledge Graph Visualization. Expert-curated biomedical knowledge graph used for hypothesis generation in computational pathology. Nodes represent biomedical entities (e.g., genes, diseases, pathways, phenotypes), and edges denote semantic or mechanistic relationships mined from literature and medical ontologies. Colors indicate entity types (see legend). A zoomed-in subgraph highlights bladder cancer-related entities and dense multi-scale connectivity enabling context-aware reasoning.

reasoning.

The final KG integrates 1,650 scientific sources (1,000 bladder cancer papers, 650 computational pathology papers, and three reference textbooks) and contains 41,053 nodes and 56,338 edges spanning biological mechanisms, clinical endpoints, and computational methods. See Figure 2.

Quality Assessment: To assess reliability, we evaluated a stratified random sample of extracted triples following established biomedical KG validation practices (Ji et al., 2021). The KG exhibits high factual grounding (99.0%) and relation accuracy (100%), with entity type accuracy improving from 64.6% to 82.5% after ontology refinement. Extended evaluation results, error analysis, and ontology details are reported in the supplementary material (Table 4).

3.2. Hypothesis Generation

To address the stochastic instability and unbounded search spaces inherent in the original *SciAgents* architecture (Ghafarollahi & Buehler, 2024), we introduce a redesigned execution model that replaces supervisor-based coordination with structured, closed-loop control. While earlier supervisor-led approaches often yielded divergent and speculative outputs, our framework enforces empirical grounding by coupling generative expansion with a formal verification stage which ensures that every synthesized hypothesis is intrinsically testable and reproducible.

3.2.1. PIPELINE OVERVIEW

The updated pipeline consists of six core agents operating in a fixed sequential order: **Path Generation** → **Ontologist** → **Scientist** → **Hypothesis Expansion** → **Novelty Critic** → **Feasibility Agent** → **Coding Agent** → **Summary Agent**. This structure eliminates the need for a central supervisor, resulting in more consistent outputs and predictable behavior across runs. A *human-in-the-loop* checkpoint was also introduced between the Scientist and Hypothesis Expansion agents, allowing domain experts to review and refine hypotheses before computational validation. This early intervention prevents resource waste on infeasible hypotheses and incorporates expert intuition that automated evaluation may miss. A detailed description of all agents, their context sources, and model assignments is provided in the Supplementary Material (Table 5).

3.2.2. PATH GENERATION AND EVALUATION

The **Path Generation Agent** traverses a biomedical knowledge graph to identify biologically meaningful multi-hop paths linking entities such as *Gene–Pathway–Disease* or *Biomarker–Tissue–Outcome*. These paths represent candidate mechanistic hypotheses, with targeted queries prioritizing under-explored or weakly connected nodes to encourage discovery beyond well-established associations.

An **Ontologist Agent** grounds each path in curated biomedical ontologies, enforcing semantic consistency and mapping symbolic relations to biologically interpretable processes (e.g., interpreting “FN1 upregulates COL1A1” as extracellular matrix remodeling in bladder cancer). This ensures that downstream reasoning operates on coherent and domain-valid hypotheses.

Each candidate path is evaluated using a multi-criteria scoring framework that balances plausibility with discovery potential. Unlike prior agentic systems that rely on single heuristics or textual self-consistency, SAGE explicitly separates plausibility-driven criteria (*Logic, Relevance*) from discovery-driven criteria (*Novelty, Surprise*), allowing controlled exploration of underexplored biological mechanisms. Specifically, SAGE assigns four complementary scores that are combined into a weighted aggregate to prioritize hypotheses for downstream validation. *Logic*, which measures semantic coherence with the query; *Relevance*, which assesses alignment with the target disease context; *Novelty*, which favors paths containing underexplored entities; and *Surprise*, which captures atypical cross-domain combinations. The four metrics are combined into a normalized weighted aggregate score,

$$S_{\text{total}} = \frac{w_{\text{logic}}S_{\text{logic}} + w_{\text{rel}}S_{\text{rel}} + w_{\text{nov}}S_{\text{nov}} + w_{\text{sur}}S_{\text{sur}}}{\sum_i w_i}, \quad (1)$$

where $w_i \geq 0$ denote metric-specific coefficients. To en-

courage discovery-oriented hypotheses, the aggregation assigns relatively larger weights to the Novelty and Surprise components. Higher weights are assigned to Novelty and Surprise to prioritize discovery-oriented hypotheses. Formal definitions of each metric are provided in Appendix B.1.

3.2.3. VALIDATION-AWARE HYPOTHESIS GENERATION AND REFINEMENT

Building on ontology-enriched graph paths, the **Scientist Agent** generates concise, dataset-aware hypotheses that are explicitly designed to be empirically testable using available cohorts such as TCGA-BLCA (Cerami et al., 2012) and institutional datasets. Unlike prior agentic systems that produce open-ended or purely conceptual hypotheses, SAGE constrains hypothesis formulation by enforcing validation feasibility at generation time.

Using a high-reasoning language model, the Scientist Agent integrates molecular, imaging, and clinical evidence to propose mechanistic relationships (e.g., linking tumor microenvironment structure to survival or therapy response). Each hypothesis follows a structured template that explicitly specifies:

- **Population:** the target patient cohort or subgroup,
- **Variables:** biological, imaging, and clinical predictors,
- **Outcome:** a measurable clinical or molecular endpoint,
- **Expected Directionality:** the hypothesized effect or interaction,
- **Validation Feasibility:** availability of required features, labels, and metadata.

Following initial formulation, hypotheses are iteratively refined through a feedback loop. A **Hypothesis Expansion Agent** enriches biological rationale and clinical interpretation, while a **Novelty Critic Agent** evaluates originality by comparing the hypothesis against existing literature using online retrieval, assigning a novelty score on a 1–10 scale. Hypotheses that fail to meet a predefined novelty threshold are revised iteratively until convergence or a maximum iteration limit is reached. This controlled refinement process improves both originality and interpretability while preserving empirical testability. Representative examples are provided in Supplementary Section E.

3.2.4. CLINICAL FEASIBILITY AGENT

To prevent validation of speculative or non-executable hypotheses, SAGE introduces a dedicated **Feasibility Agent** that performs an explicit feasibility assessment prior to empirical testing. Unlike prior agentic systems (Ghafarollahi &

Buehler, 2024) (Vaidya et al., 2025) that implicitly assume data and tool availability, the Feasibility Agent enforces validation realism as a first-class constraint.

Each candidate hypothesis is evaluated using a four-step verification protocol that assesses: (1) *data availability* (35%), (2) *technical readiness and tool maturity* (25%), (3) *logical soundness and falsifiability* (25%), and (4) *computational and timeline constraints* (15%). These criteria are combined into a weighted feasibility score and a categorical verdict (e.g., *feasible*, *conditionally feasible*, *infeasible*).

Crucially, feasibility assessment is grounded in external, verifiable resources rather than purely textual reasoning. The agent queries biomedical literature, public omics repositories, clinical trial registries, and software ecosystems to confirm the existence of suitable datasets, mature analysis tools, and realistic execution pathways. By filtering hypotheses that lack concrete data or tooling support, the Feasibility Agent reduces wasted computation and increases the likelihood that retained hypotheses can be empirically validated. Detailed scoring criteria and external resources are summarized in Supplementary Tables 6 and 7.

3.2.5. MULTI-CRITIC NOVELTY EVALUATION

To provide robust and calibrated novelty assessments, we implement a game-theoretic multi-critic evaluation framework inspired by adversarial debate protocols (Irving et al., 2018). This approach simulates the peer review process through structured argumentation among three agents with distinct epistemic stances: a Prover (optimistic) that advocates for the hypothesis’s novelty by identifying unique mechanistic claims and gaps in existing literature; a Verifier (conservative) that challenges novelty claims by retrieving contradicting or overlapping prior work; and a Judge (balanced) that synthesizes arguments from both sides and renders a final assessment.

Each critic grounds its assessment in real-time literature retrieval across six scholarly databases (PubMed, Semantic Scholar, Europe PMC, bioRxiv, arXiv, and CrossRef). The Verifier specifically searches for prior work that may refute the Prover’s novelty claims, providing DOI-linked citations for transparency.

Initial scores are collected from each critic on a 1–10 scale. When significant disagreement is detected (standard deviation $\sigma > 1.0$), a multi-round Bayesian debate (Zhang et al., 2024) is initiated. Each round proceeds in three steps: the Prover presents key novelty claims with a proposed score and confidence level; the Verifier searches for refuting literature and responds with counter-evidence; and the Judge evaluates both arguments and provides a synthesized assessment. Scores update iteratively based on each agent’s confidence-weighted proposals until convergence ($\sigma < 0.5$)

or a maximum of three rounds. To penalize superficially novel but actually incremental claims, the Verifier can flag arguments as *specious*—claims that appear novel but are directly refuted by existing literature—triggering a score penalty when upheld by the Judge.

The final novelty score is computed as an unweighted mean across all three critics, treating the Prover, Verifier, and Judge assessments with equal importance. More details available in the supplementary section D.

3.3. Empirical Hypothesis Validation

A central contribution of SAGE is a validation-first execution framework that transforms generated hypotheses into reproducible empirical evidence. This is implemented through a dedicated **Validation Stage** composed of three coordinated agents: **Coding Instructions Agent** → **Coding Agent** → **Coding Results Interpreter**. Together, these agents form a closed validation loop that compiles high-level scientific hypotheses into executable analyses and interpretable results.

Unlike prior LLM-based code agents that execute predefined tasks or static scripts, the **Coding Agent** in SAGE dynamically synthesizes and executes task-specific analysis code conditioned on the hypothesis structure, dataset availability, and validation requirements. This enables direct empirical testing of arbitrary hypotheses over real patient cohorts while enforcing reproducibility and execution safety.

3.3.1. ARCHITECTURE AND CONTROL FLOW

The Coding Agent consists of three cooperating sub-agents orchestrated by a central controller:

- **Task Agent:** Translates structured specifications from the Coding Instructions Agent (e.g., hypothesis variables, cohort definitions, endpoints) into a normalized execution plan.
- **Data Agent:** Resolves dataset locations from the laboratory data bank, performs feature extraction via registered tools, and returns analysis-ready inputs with full provenance metadata.
- **Validation Agent:** Compiles and executes the analysis plan in a secure sandbox, producing structured outputs such as tables, plots, and performance metrics.

Execution is bounded to at most N feedback-driven iterations, after which unresolved cases are escalated for expert review. All results, logs, and artifacts are forwarded to the Coding Results Interpreter for feasibility scoring and integration into the overall discovery pipeline.

3.3.2. HYPOTHESIS VALIDATION PIPELINE

All Coding Agent sub-components run in containerized, sandboxed environments with strict resource limits and read-only host access, ensuring safe and reproducible execution. The Coding Agent interfaces with a shared registry of validated laboratory tools spanning computational pathology (e.g., patch extraction, segmentation, detection, foundation models, tertiary lymphoid structure (TLS) detection and collagen analysis) and clinical oncology (e.g., survival modeling, Kaplan–Meier analysis, concordance evaluation).

Each tool is described using a standardized interface specifying inputs, outputs, execution constraints, and resource requirements, enabling automatic selection and composition. When no suitable tool is available, the Coding Agent synthesizes new Python code to complete the requested analysis while adhering to sandbox constraints. Tool discovery, selection, and execution are mediated by a unified tool orchestration subsystem described in the supplementary material (Appendix B.4, Figure 5).

4. Results

We evaluate SAGE by demonstrating end-to-end discovery of novel, interpretable, molecularly driven prognostic biomarkers, from literature grounding and feasibility assessment to novelty evaluation and empirical validation on public cohorts. We further analyze design choices, benchmark against prior frameworks, and assess novelty calibration.

4.1. End-to-End Biomarkers Discovery

We demonstrate the end-to-end capability of SAGE through a representative hypothesis that was autonomously generated, assessed as high novelty and high clinical feasibility, and empirically validated on a public cohort. Starting from literature-grounded reasoning, SAGE identified a previously underexplored joint prognostic interaction between a molecular biomarker, FABP5 (E-FABP) expression, and an imaging-derived immune spatial phenotype, the abundance of TLS-like lymphoid aggregates on whole-slide images in bladder cancer.

SAGE translated this hypothesis into an executable validation specification, jointly stratifying patients in TCGA-BLCA by FABP5 expression and TLS abundance, and evaluating overall survival and lymph-node positivity. Automated survival analysis revealed clear prognostic separation between patient groups, with high FABP5 expression combined with scarce TLS-like aggregates associated with significantly worse overall survival compared to low FABP5 expression with abundant TLS-like aggregates (Fig. 3). Cox proportional hazards modeling further confirmed elevated risk in the high-FABP5/low-TLS group.

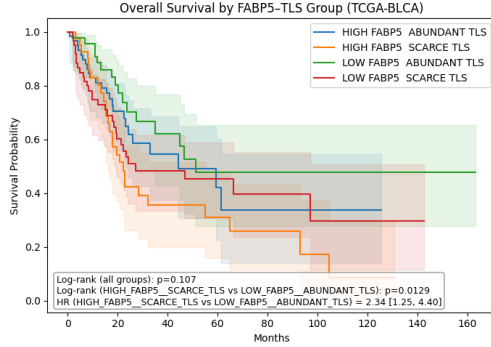


Figure 3. Pathology-informed overall survival analysis for joint FABP5-TLS stratification in TCGA-BLCA. Patients with high FABP5 expression and scarce TLS-like lymphoid aggregates on whole-slide pathology images exhibit significantly worse overall survival compared to patients with low FABP5 expression and abundant TLS-like aggregates.

This result illustrates how SAGE unifies hypothesis generation, biological interpretation across modalities, novelty and feasibility assessment, and empirical hypothesis validation within a single pipeline. Importantly, the discovered biomarker is not only statistically supported but also biologically interpretable and clinically actionable, addressing key barriers to clinical adoption. Full agentic execution details are provided in the Supplementary Material (Sec. E.5).

4.2. Design Choices

We analyze how key design choices in SAGE affect hypothesis quality, empirical reliability, and computational efficiency. Specifically, we evaluate (i) prompt refinement strategies for reducing hallucinations and improving scientific consistency, and (ii) memory allocation and inter-agent communication protocols to characterize the trade-off between hypothesis quality and inference cost.

Prompt Refinement and Domain Adaptation: Baseline agentic frameworks exhibited verbose outputs and unsupported quantitative claims. Incorporating negative prompting (Qiao et al., 2024) to discourage speculative assertions, together with few-shot prompting to standardize structure, substantially reduced hallucinations and improved consistency across runs. These strategies yielded concise, reproducible hypotheses with lower token usage. Representative pre- and post-refinement examples are provided in the Supplementary Material (Sec. E.3).

Memory and Pipeline Architecture: We compared a *shared-memory, chat-based pipeline* (CP), in which all agents access the full conversation history, with a *specific-memory, graph-based pipeline* (GP), where each agent receives only task-relevant context from its immediate predecessor. For more details check section C in the supplementary material.

As summarized in Table 1, GP reduced prompt tokens by 57.5% and completion tokens by 14.9%, corresponding to a 25–75% reduction in inference cost, while maintaining comparable runtime and hypothesis novelty (7/10 vs. 8/10). These results indicate that targeted context allocation preserves discovery quality while enabling predictable, scalable execution.

Table 1. Comparison of graph-based (GP) and chat-based (CP) pipelines on TCGA-BLCA runs.

Metric	GP	CP	$\Delta(\%)$
Prompt (\pm SD)	$9,002 \pm 2,367$	$21,210 \pm 3,146$	-57.5
Completion (\pm SD)	$10,011 \pm 2,909$	$11,765 \pm 817$	-14.9
Time sec. (\pm SD)	222.15 ± 72.98	227.23 ± 29.23	-2.2
Novelty	7 / 10	8 / 10	-12.5
Rel. Cost	1x	1.3–4x	75 \downarrow

4.3. Comparison of Hypothesis Generation Pipelines

We quantitatively compared SAGE against two commonly used hypothesis-generation baselines to assess hypothesis novelty, inter-reviewer agreement, and evidence-retrieval behavior under a controlled evaluation setting, as novelty is the only evaluation dimension shared by pipelines that lack the ability to empirically validate generated hypotheses. The evaluated pipelines were: (i) a *single-response LLM* baseline, in which a single large language model generates one hypothesis per run (ChatGPT 5.1); (ii) an *agent-flow* (Li et al., 2025) consisting of a multi-agent, iterative workflow with explicit web browsing; and (iii) SAGE (ours), which generates hypotheses via structured traversal of a domain-specific knowledge graph. All pipelines were prompted with an identical task: “*Identify a novel research hypothesis linking tertiary lymphoid structures (TLS) and genes in bladder cancer.*”

Each pipeline was executed independently for 10 runs, yielding a total of 30 hypotheses. All outputs were evaluated using the same LLM-based novelty scoring ensemble, which independently queried external scientific literature (Semantic Scholar, PubMed, and arXiv) and produced aggregated quantitative metrics. Specifically, we report: *mean_reviews* (average novelty score across reviewers), *consensus_score* (inter-reviewer agreement), and *total_unique_references* (number of distinct literature sources retrieved during evaluation).

Table 2 summarizes the results averaged across runs (mean \pm standard deviation). Across pipelines, novelty and agreement scores were broadly comparable. SAGE achieved a slightly higher mean novelty score and consensus score on average, albeit with increased variability across runs. In contrast, SAGE retrieved substantially fewer unique literature references during evaluation.

Table 2. Comparison of hypothesis-generation pipelines (10 runs each). Values are reported as mean \pm standard deviation.

Metric	LLM	Agent Flow	SAGE
Novelty (mean_rev.)	7.0 \pm 0.7	7.1 \pm 0.5	7.3 \pm 1.0
Consensus	7.1 \pm 0.9	7.1 \pm 0.6	7.3 \pm 1.0
Refs. retrieved	6.0 \pm 1.1	5.2 \pm 1.4	2.4 \pm 1.7

SAGE preserves hypothesis novelty and internal agreement while achieving substantially greater computational efficiency by relying on structured relational reasoning rather than retrieval-heavy workflows.

4.4. Novelty Calibration via Multi-Critic Deliberation

We evaluate whether *explicit adversarial deliberation*—iterative, evidence-driven score revision triggered by critic disagreement—improves the calibration of scientific novelty assessment beyond multi-critic averaging. All experiments use time-travel backtesting on historical proposals to prevent temporal leakage (Ye et al., 2026).

Novelty spectrum and experimental design: We categorize proposal novelty using a five-tier scale. At the highest tier A, lies foundational breakthroughs that introduce new paradigms. Tiers B and C represent high-innovation and significant non-paradigmatic contributions, respectively. Tier D consists of incremental extensions to existing baselines, while Tier E identifies proposals with significant technical flaws or previously refuted claims. We compare four configurations that isolate the effect of deliberation while holding all other factors constant: (i) a *Single-Critic* baseline; (ii) a *Two-Critic* ensemble (Prover+Verifier) without interaction; (iii) a *Multi-Critic (No Debate)* setting where three critics independently score proposals and are averaged; and (iv) *Multi-Critic (Full)*, in which critics enter an iterative debate only when initial disagreement exceeds a threshold ($\sigma > 1.0$). Thus, the sole difference between (iii) and (iv) is disagreement-triggered deliberation.

Effect of deliberation on novelty separability: Table 3 reports overall accuracy and the A–E separability, defined as the mean score difference between the extremes of the novelty spectrum. While independent critics improves performance, enabling deliberation yields the largest marginal gain: a 1.76-point increase in A–E separability over the no-debate condition, demonstrating that deliberation improves calibration beyond critic diversity or score averaging.

When and why deliberation helps: Deliberation primarily benefits proposals near the extremes of the novelty spectrum, where naive averaging tends to compress scores toward the center. Debate is triggered most frequently for breakthrough (A) and specious (E) cases, where critics initially disagree on whether apparent novelty reflects genuine conceptual advances or superficial reformulations. Detailed per-category deliberation statistics are provided in the Sup-

Table 3. Effect of deliberation on novelty separability. A–E Gap denotes the mean score difference between breakthrough (A) and specious (E) proposals.

Configuration	Accuracy	A–E Gap
Single-Critic	56.0%	1.12
Two-Critic (Verifier+Prover)	75.3%	4.18
Multi-Critic (No Debate)	81.3%	5.02
Multi-Critic (Full)	91.3%	6.78

plementary Material D.

Representative cases: Tier A (Breakthrough): AlphaFold2 (Jumper et al., 2021). Evaluated as of December 2019 using only prior literature, AlphaFold2 initially exhibited critic disagreement ($\sigma = 1.31$) over whether its contribution was incremental or mechanistically novel. Through deliberation, critics exchanged evidence on architectural design and prior art, including Evoformer-based joint MSA–structure reasoning and geometric consistency constraints, converging to a final novelty score of 9.5. This case illustrates how deliberation resolves ambiguity using contemporaneous evidence rather than retrospective judgment.

Tier E (Specious): STAP Cells (Obokata et al., 2014). Evaluated in June 2014 post-retraction, STAP Cells showed substantial initial disagreement ($\sigma = 2.07$; Prover: 6.2, Verifier: 2.1). During deliberation, the Verifier identified eight refutation papers and three failed replications documenting data fabrication. The Judge distinguished mechanistic plausibility from empirical validity, yielding a final consensus score of 1.5 and demonstrating how deliberation suppresses superficially novel but invalid claims.

Computational cost: Deliberation increases evaluation cost by $3.75 \times$ relative to a single critic (\$0.15 vs. \$0.04 per proposal), yielding a 35.3% absolute accuracy gain. This corresponds to approximately \$0.004 per percentage point of accuracy improvement, representing a reasonable tradeoff for high-stakes novelty assessment.

5. Conclusion

We presented SAGE, a structured agentic framework for end-to-end scientific hypothesis discovery and evaluation, designed to support reproducible and scalable discovery in computational pathology. Through design choices in prompting, memory allocation, and pipeline architecture, SAGE generates concise, evidence-grounded hypotheses and translates them into executable validation analyses linking image-derived pathology features with molecular and clinical endpoints, while substantially reducing computational cost. Comparative evaluation shows that SAGE achieves hypothesis novelty comparable to retrieval-heavy and multi-agent baselines, despite relying on structured, pathology-aware reasoning rather than exhaustive external

search. We further demonstrated that multi-critic deliberation significantly improves the calibration and separability of novelty judgments. Together, these results position SAGE as a practical and extensible system for end-to-end hypothesis discovery, interpretation, and validation in computational pathology at scale.

Impact Statement

This work aims to advance automated scientific discovery by enabling structured, validation-first hypothesis generation grounded in real biomedical data. By integrating computational pathology and clinical datasets, SAGE may support researchers in identifying prognostic and predictive biomarkers more efficiently. However, the system is not intended to provide clinical decision-making or patient-level recommendations, and all generated hypotheses require expert interpretation and independent validation prior to any translational or clinical use. As with all data-driven systems, potential risks include biases present in source datasets and knowledge bases, underscoring the importance of diverse data curation and careful evaluation. Overall, we believe the benefits of improving reproducibility and empirical grounding in scientific reasoning outweigh potential risks when the system is used responsibly within research settings.

References

Agrawal, L. A., Tan, S., Soylu, D., Ziems, N., Khare, R., Opsahl-Ong, K., Singhvi, A., Shandilya, H., Ryan, M. J., Jiang, M., Potts, C., Sen, K., Dimakis, A. G., Stoica, I., Klein, D., Zaharia, M., and Khattab, O. Gepa: Reflective prompt evolution can outperform reinforcement learning, 2025. URL <https://arxiv.org/abs/2507.19457>.

Anthropic. Model context protocol. <https://modelcontextprotocol.io>, 2024. Technical specification for standardized tool and context interfaces for large language model agents.

Belova, M., Xiao, J., Tuli, S., and Jha, N. K. Graphmert: Efficient and scalable distillation of reliable knowledge graphs from unstructured data, 2025. URL <https://arxiv.org/abs/2510.09580>.

Bodenreider, O. The unified medical language system (umls): integrating biomedical terminology. *Nucleic acids research*, 32(suppl_1):D267–D270, 2004.

Brandes, U., Eiglsperger, M., Herman, I., Himsolt, M., and Marshall, M. S. GraphML progress report: Structural layer proposal. In *Graph Drawing*, pp. 501–512, 2001.

Buehler, M. J. Accelerating scientific discovery with generative knowledge extraction, graph-based representa-

tion, and multimodal intelligent graph reasoning. *Machine Learning: Science and Technology*, 2024. doi: 10.1088/2632-2153/ad67db.

Cerami, E., Gao, J., Dogrusoz, U., Gross, B. E., Sumer, S. O., Aksoy, B. A., Jacobsen, A., Byrne, C. J., Heuer, M. L., Larsson, E., et al. The cbio cancer genomics portal: An open platform for exploring multidimensional cancer genomics data. *Cancer Discovery*, 2(5):401–404, 2012.

Gandhi, S., Shah, D., Patwardhan, M., Vig, L., and Shroff, G. Researchcodeagent: An llm multi-agent system for automated codification of research methodologies, 2025. URL <https://arxiv.org/abs/2504.20117>.

Ghafarollahi, A. and Buehler, M. J. Sciagents: Automating scientific discovery through multi-agent intelligent graph reasoning, 2024. URL <https://arxiv.org/abs/2409.05556>.

Hagberg, A., Swart, P., and Schult, D. A. Exploring network structure, dynamics, and function using networkx. In *Proceedings of the 7th Python in Science Conference*, pp. 11–15, 2008.

Hillerstrom, F. and Burghouts, G. Towards probabilistic inductive logic programming with neurosymbolic inference and relaxation, 2024. URL <https://arxiv.org/abs/2408.11367>.

Himmelstein, D. S., Lizee, A., Hessler, C., Brueggeman, L., Chen, S. L., Hadley, D., Green, A., Khankhanian, P., and Baranzini, S. E. Systematic integration of biomedical knowledge prioritizes drugs for repurposing. *eLife*, 6: e26726, 2017.

Irving, G., Christiano, P., and Amodei, D. Ai safety via debate, 2018. URL <https://arxiv.org/abs/1805.00899>.

Ji, S., Pan, S., Cambria, E., Marttinen, P., and Yu, P. S. A survey on knowledge graphs: Representation, acquisition, and applications. *IEEE Transactions on Neural Networks and Learning Systems*, 33(2):494–514, 2021. doi: 10.1109/TNNLS.2020.2978386.

Jumper, J., Evans, R., Pritzel, A., Green, T., Figurnov, M., Ronneberger, O., Tunyasuvunakool, K., Bates, R., Žídek, A., Potapenko, A., Bridgland, A., Meyer, C., Kohl, S. A. A., Ballard, A. J., Cowie, A., Romera-Paredes, B., Nikolov, S., Jain, R., Adler, J., Back, T., Petersen, S., Reiman, D., Clancy, E., Zielinski, M., Steinegger, M., Pacholska, M., Berghammer, T., Bodenstein, S., Silver, D., Vinyals, O., Senior, A., Kavukcuoglu, K., Kohli, P., and Hassabis, D. Highly accurate protein structure prediction with AlphaFold. *Nature*, 596(7873):583–589, 2021. doi: 10.1038/s41586-021-03819-2.

Li, Z., Zhang, H., Han, S., Liu, S., Xie, J., Zhang, Y., Choi, Y., Zou, J., and Lu, P. In-the-flow agentic system optimization for effective planning and tool use, 2025. URL <https://arxiv.org/abs/2510.05592>.

Lu, M. Y., Chen, B., Williamson, D. F., Chen, R. J., Zhao, M., Chow, A. K., Ikemura, K., Kim, A., Pouli, D., Patel, A., et al. A multimodal generative ai copilot for human pathology. *Nature*, 634(8033):466–473, 2024.

Luo, R., Sun, L., Xia, Y., Qin, T., Zhang, S., Poon, H., and Liu, T.-Y. BioGPT: generative pre-trained transformer for biomedical text generation and mining. *Briefings in Bioinformatics*, 23(6), September 2022. ISSN 1477-4054. doi: 10.1093/bib/bbac409. URL <http://dx.doi.org/10.1093/bib/bbac409>.

Lyu, X., Liang, Y., Chen, W., Ding, M., Yang, J., Huang, G., Zhang, D., He, X., and Shen, L. Wsi-agents: A collaborative multi-agent system for multi-modal whole slide image analysis. *arXiv preprint arXiv:2507.14680*, 2025.

Niu, S., Yang, K., Zhao, R., Liu, Y., Li, Z., Wang, H., and Chen, W. Tree-KG: An expandable knowledge graph construction framework for knowledge-intensive domains. In Che, W., Nabende, J., Shutova, E., and Pilehvar, M. T. (eds.), *Proceedings of the 63rd Annual Meeting of the Association for Computational Linguistics (Volume 1: Long Papers)*, pp. 18516–18529, Vienna, Austria, July 2025. Association for Computational Linguistics. ISBN 979-8-89176-251-0. doi: 10.18653/v1/2025.acl-long.907. URL <https://aclanthology.org/2025.acl-long.907/>.

Obokata, H., Wakayama, T., Sasai, Y., Kojima, K., Vacanti, M. P., Niwa, H., Yamato, M., and Vacanti, C. A. Retracted article: Stimulus-triggered fate conversion of somatic cells into pluripotency. *Nature*, 505(7485):641–647, 2014.

Ouzzani, M., Hammady, H., Fedorowicz, Z., and Elmagarmid, A. Rayyan—a web and mobile app for systematic reviews. *Systematic Reviews*, 5(1):210, 2016. doi: 10.1186/s13643-016-0384-4.

Park, J. S., O’Brien, J. C., Cai, C. J., Morris, M. R., Liang, P., and Bernstein, M. S. Generative agents: Interactive simulacra of human behavior, 2023. URL <https://arxiv.org/abs/2304.03442>.

Peng, N., Poon, H., Quirk, C., Toutanova, K., and Yih, W.-t. Cross-sentence n-ary relation extraction with graph lstms. *Transactions of the Association for Computational Linguistics*, 5:101–115, 2017.

Qiao, S., Xv, N., Liu, B., and Geng, X. Negative-prompt-driven alignment for generative language model, 2024. URL <https://arxiv.org/abs/2410.12194>.

Reimers, N. and Gurevych, I. Sentence-bert: Sentence embeddings using siamese bert-networks. In *Proceedings of the 2019 Conference on Empirical Methods in Natural Language Processing and the 9th International Joint Conference on Natural Language Processing*, pp. 3982–3992, 2019. doi: 10.18653/v1/D19-1410.

Remy, F., Demuynck, K., and Demeester, T. Biolord: Learning ontological representations from definitions (for biomedical concepts and their textual descriptions), 2022. URL <https://arxiv.org/abs/2210.11892>.

Singhal, K., Tu, T., Gottweis, J., Sayres, R., Wulczyn, E., Hou, L., Clark, K., Pfohl, S., Cole-Lewis, H., Neal, D., Schaeckermann, M., Wang, A., Amin, M., Lachgar, S., Mansfield, P., Prakash, S., Green, B., Dominowska, E., y Arcas, B. A., Tomasev, N., Liu, Y., Wong, R., Semturs, C., Mahdavi, S. S., Barral, J., Webster, D., Corrado, G. S., Matias, Y., Azizi, S., Karthikesalingam, A., and Natarajan, V. Towards expert-level medical question answering with large language models, 2023. URL <https://arxiv.org/abs/2305.09617>.

Vaidya, A. J., Meissen, F., Castro, D. C., Bannur, S., Lazard, T., Williamson, D. F. K., Mahmood, F., Alvarez-Valle, J., Hyland, S. L., and Bouzid, K. Nova: An agentic framework for automated histopathology analysis and discovery, 2025. URL <https://arxiv.org/abs/2511.11324>.

Xiao, S., Liu, Z., Zhang, P., and Muennighoff, N. Bge: Baai general embedding. GitHub repository, 2023. URL <https://github.com/FlagOpen/FlagEmbedding>.

Yao, S., Yu, D., Zhao, J., Shafran, I., Griffiths, T. L., Cao, Y., and Narasimhan, K. Tree of thoughts: Deliberate problem solving with large language models, 2023. URL <https://arxiv.org/abs/2305.10601>.

Ye, B., Chen, S., Tu, J., Liu, C., Xiong, Z., Schmidgall, S., and Bitterman, D. S. Proof of time: A benchmark for evaluating scientific idea judgments, 2026. URL <https://arxiv.org/abs/2601.07606>.

Zhang, W., Zang, C., and Kainz, B. Truth or deceit? a Bayesian decoding game enhances consistency and reliability, 2024. URL <https://arxiv.org/abs/2410.01064>.

Zhang, Y., Zheng, W., Lin, H., Wang, J., Yang, Z., and Dumontier, M. Drug-drug interaction extraction via hierarchical rnns on sequence and shortest dependency

paths. *Bioinformatics*, 34(5):828–835, 2018. doi: 10.1093/bioinformatics/btx546.

Zhang, Y., Sui, X., Pan, F., Yu, K., Li, K., Tian, S., Erdengasileng, A., Han, Q., Wang, W., Wang, J., et al. A comprehensive large-scale biomedical knowledge graph for ai-powered data-driven biomedical research. *Nature Machine Intelligence*, pp. 1–13, 2025.

Zhou, Y., Liu, H., Srivastava, T., Mei, H., and Tan, C. Hypothesis generation with large language models. In *Proceedings of the 1st Workshop on NLP for Science (NLP4Science)*, pp. 117–139. Association for Computational Linguistics, 2024. doi: 10.18653/v1/2024.nlp4science-1.10. URL <http://dx.doi.org/10.18653/v1/2024.nlp4science-1.10>.

A. Knowledge Graph Construction Details

This section provides additional implementation details, ontology specifications, and quality analyses for the knowledge graph (KG) construction pipeline described in Section 3.1.

A.1. Paper Screening and Scoring

Candidate papers are retrieved using domain-specific keyword queries covering computational pathology, disease biomarkers, spatial analysis, and whole-slide imaging. Each paper is scored using a composite metric combining keyword frequency, semantic proximity, SapBERT similarity, and journal impact factor. Thresholds are calibrated empirically to balance recall and precision, resulting in approximately 40% of retrieved papers being excluded as insufficiently relevant.

A.2. Text Extraction and Preprocessing

PDF text extraction employs a three-tier fallback strategy using `pdfplumber`, `PyMuPDF`, and `pypdf` to accommodate heterogeneous document formats. Extracted text is normalized and segmented into overlapping chunks of approximately 1,500 tokens to preserve local semantic context for relation extraction.

A.3. Triple Extraction and Ontology Normalization

Triple extraction is performed using `GPT-4o-mini` with structured prompts designed to enforce entity typing, relation normalization, and evidence attribution. Relation phrases are mapped to canonical forms using ontology-aligned rule-based normalization (Peng et al., 2017; Zhang et al., 2018). Triples with confidence scores below 0.5 are discarded.

The ontology schema includes fine-grained entity types such as *Gene*, *Pathway*, *Disease*, *ClinicalEndpoint*, *TissueRegion*, *StainingMethod*, and *Algorithm*. Disambiguation rules are applied to resolve patient cohorts, clinical outcomes, and gene identifiers.

A.4. Local and Global Graph Construction

For each document d , a local graph $G(d) = (V(d), E(d))$ is constructed, where nodes correspond to unique entities and edges aggregate all triples linking entity pairs. Edge weights are defined as the maximum confidence among supporting triples.

Local graphs are fused into a global KG using BGE-Large embeddings (Xiao et al., 2023). Nodes are merged when cosine similarity exceeds $\tau = 0.9$, and redundant edges are merged by summing weights. Disconnected components with fewer than three nodes are pruned. Graphs are serialized in GraphML format for interoperability (Brandes et al., 2001; Hagberg et al., 2008). See figure 2

A.5. Knowledge Graph Quality Evaluation

KG quality is assessed via stratified random sampling of 200 triples across relation types. Each triple is evaluated along three dimensions: (1) factual grounding with respect to the cited evidence span, (2) correctness of entity names and types, and (3) accuracy and directionality of the extracted relation.

Initial evaluation yielded 99.0% factual grounding and 100% relation accuracy, with lower entity type accuracy (64.6%) due to systematic ontology ambiguities. Following ontology refinement and post-processing validation, re-evaluation on a held-out sample achieved 82.5% strict and 92.5% lenient entity type accuracy. Detailed results are summarized in Table 4.

Table 4. Knowledge Graph Extraction Quality Assessment

Metric	Initial Pipeline	Refined Pipeline
Factual Grounding	99.0%	99.0%
Relation Accuracy	100.0%	100.0%
Entity Type Accuracy (Strict)	64.6%	82.5%
Entity Type Accuracy (Lenient)	99.0%	92.5%
Hallucination Rate	0.5%	<1.0%

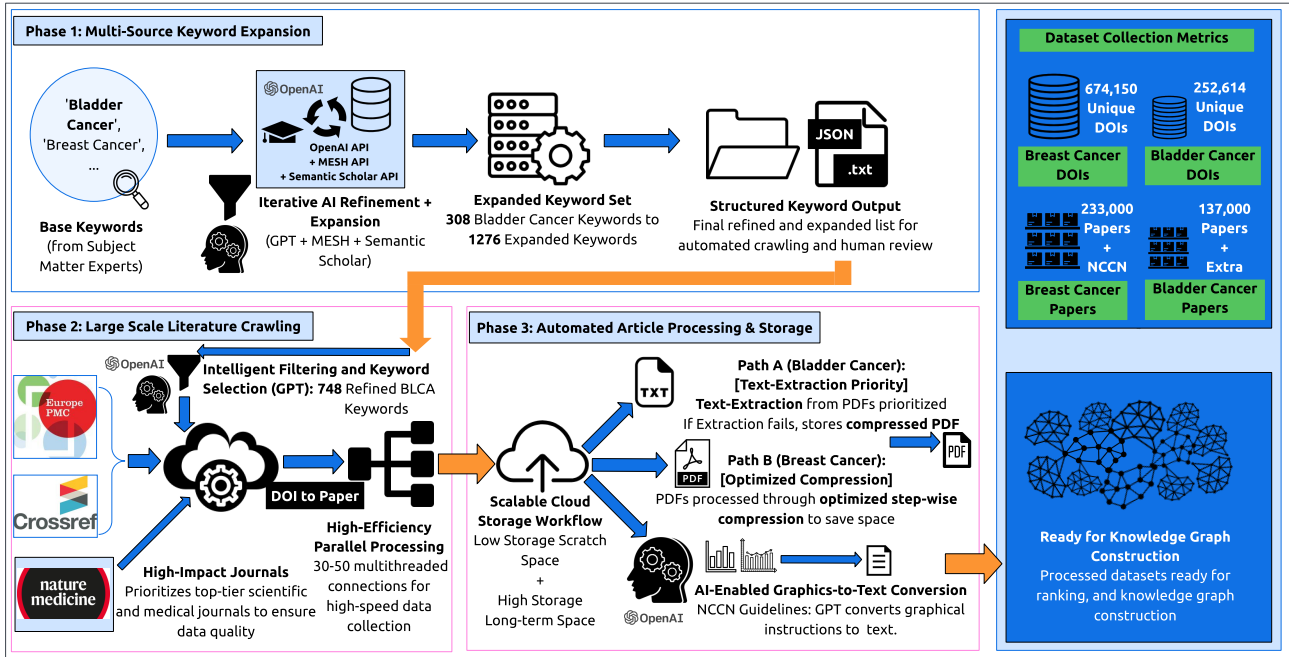


Figure 4. Overview of the AI-Enabled Literature Processing and Knowledge Graph Construction Workflow. Visualization of a three-phase workflow for AI-enabled data collection and processing: Phase 1: Keyword Expansion using OpenAI, MESH, and Semantic Scholar APIs, Phase 2: Large Scale Literature Crawling from high-impact sources, and Phase 3: Automated Article Processing and Storage via text extraction prioritization with optimized compression, for preparing the dataset for knowledge graph construction.

A.6. Limitations

Remaining challenges include entity boundary delineation for complex noun phrases, disambiguation of clinical endpoints, and separation of visualization methods from software tools. These limitations motivate future integration of ontology-constrained classifiers and external biomedical resources such as UMLS (Bodenreider, 2004).

B. Hypothesis Generation Pipeline Details

This section provides extended methodological details complementing Section 3 of the main text.

B.1. Path-Level Evaluation Metrics

This subsection provides formal definitions of the four path-level evaluation metrics (*Logic*, *Relevance*, *Novelty*, and *Surprise*) introduced in Section 3.2.2.

B.1.1. LOGIC SCORE

The Logic score assesses whether a candidate path forms a semantically coherent explanation of the user query, with the goal of filtering out paths that contain conceptual gaps or implausible transitions. To compute this score, each path P is first converted into a natural-language sentence by concatenating its constituent entities and relations in their traversal order. Both the user query Q and the resulting path description are then embedded into a shared semantic space. Let $\mathbf{v}_{\text{query}}$ denote the embedding of the query and \mathbf{v}_{path} denote the embedding of the path description. The Logic score is defined as the cosine similarity between these two vectors:

$$\text{Score}_{\text{logic}} = \text{CosSim}(\mathbf{v}_{\text{query}}, \mathbf{v}_{\text{path}}).$$

Higher values indicate stronger semantic alignment between the path and the query, whereas lower values typically correspond to semantic breaks or loosely connected entity chains.

B.1.2. RELEVANCE SCORE

While the Logic score focuses on internal coherence, the Relevance score measures how closely a path aligns with the target research domain, such as a specific disease context. Each entity e_i in a path $P = \{e_1, \dots, e_N\}$ is represented by a normalized embedding vector \mathbf{e}_i , and the target domain is represented by a normalized embedding vector $\mathbf{c}_{\text{target}}$. Relevance is quantified by computing the average Euclidean distance between the path entities and the domain center in embedding space:

$$\text{Score}_{\text{rel}} = 1 - \frac{1}{N} \sum_{i=1}^N \|\mathbf{e}_i - \mathbf{c}_{\text{target}}\|_2.$$

The resulting value is linearly rescaled and clamped to the interval $[0, 1]$ to ensure numerical stability and comparability across paths. Paths whose entities cluster near the domain center receive higher relevance scores, reflecting stronger topical alignment with the target research focus.

B.1.3. NOVELTY SCORE

To encourage discovery beyond well-established associations, SAGE incorporates a Novelty score that favors paths containing rare or underexplored entities in the knowledge graph. Let $\deg(e)$ denote the degree of entity e in the global knowledge graph $G = (V, E)$. An empirical occurrence probability for each entity is defined as:

$$P(e) = \frac{\deg(e) + \epsilon}{\sum_{v \in V} \deg(v) + \epsilon},$$

where ϵ is a small constant introduced to avoid division by zero. The information content of an entity is given by $-\log P(e)$, which assigns higher values to entities with lower graph degree. The Novelty score of a path is computed as the average information content of its constituent entities:

$$\text{Score}_{\text{nov}} = \frac{1}{|P|} \sum_{e \in P} -\log P(e).$$

To ensure comparability across candidate paths, this score is further normalized using min–max scaling. As a result, paths that include less-connected or less-studied entities are assigned higher novelty scores.

B.1.4. SURPRISE SCORE

Complementing entity-level novelty, the Surprise score captures the extent to which a path deviates from conventional domain patterns by forming atypical cross-domain connections. Each entity in the knowledge graph belongs to a semantic category (e.g., Gene, Disease, Phenotype), allowing a categorical distribution to be defined for any given path. Let $P_{\text{actual}}(c)$ denote the empirical category distribution of entities within a path, and let $P_{\text{expected}}(c)$ denote the corresponding category distribution over the entire knowledge graph. Surprise is quantified using the Kullback–Leibler divergence between these two distributions:

$$\text{Score}_{\text{surprise}} = \text{KL}(P_{\text{actual}} \parallel P_{\text{expected}}),$$

where

$$\text{KL}(P \parallel Q) = \sum_c P(c) \log \frac{P(c)}{Q(c)}.$$

The resulting divergence values are normalized to the interval $[0, 1]$ across all candidate paths. Higher Surprise scores indicate paths that combine entity categories in unexpected ways, potentially highlighting unconventional mechanistic hypotheses.

B.1.5. WEIGHTED AGGREGATION

The four normalized metrics are combined into a single composite score to facilitate ranking and selection. Specifically, each path is assigned a weighted aggregate score:

$$\text{Score}_{\text{total}} = w_{\text{logic}} S_{\text{logic}} + w_{\text{rel}} S_{\text{rel}} + w_{\text{nov}} S_{\text{nov}} + w_{\text{sur}} S_{\text{sur}},$$

where the weights satisfy $\sum_i w_i = 1$. In our experiments, higher weights are assigned to Novelty and Surprise to emphasize discovery-oriented criteria. Candidate paths are ranked in descending order according to $\text{Score}_{\text{total}}$, and the top-ranked paths are forwarded to subsequent hypothesis formulation and validation stages.

B.2. Agent Workflow and Role Allocation

This subsection includes the complete **Agent Workflow Table** (Table 5), which outlines the role, context source, and model assignment for each agent in the hypothesis-generation pipeline. These details clarify how responsibilities are distributed across agents and how the overall pipeline achieves modularity and reproducibility.

Table 5. Complete Agent Workflow. Each agent is defined by its context source (graph-based pipeline(GP)), model, role, and model-selection rationale. The Coding Agent is described separately in Section 2.3 of the main text.

Agent	Context (GP)	Source	Model	Role	Model-Selection Rationale
Path Generation Agent	N/A pipeline	(starts	GPT-5 Nano	Generate paths between nodes in the knowledge graph by querying and traversing relationships.	Cheapest model; task requires only tool calling (knowledge-graph queries) and minimal reasoning.
Ontologist	Path Generation Agent	Generation	GPT-5 Mini	Define technical terms and articulate biological or clinical relationships in the generated paths.	Balanced model; requires domain knowledge and clarity of explanation but not maximal reasoning.
Scientist	Ontologist		GPT-5 (high reasoning)	Craft concise, scientifically rigorous, dataset-specific hypotheses that can be validated with available data.	Best available model; critical reasoning task determining overall hypothesis quality.
Hypothesis Expansion Agent	Scientist, Ontologist	Ontolo-	GPT-5 Mini	Expand the hypothesis with improvements, relevant background, scientific rationale, and potential implications.	Balanced model; competence needed, but conciseness valued over maximal reasoning.
Novelty Critic Agent	Hypothesis Expansion Agent	Expan-	GPT-5 Mini	Search online resources for similar publications, compare similarities and differences, and assign a novelty score (1–10).	Balanced model; requires literature-search capability and comparative analysis.
Coding Instructions Agent	Hypothesis Expansion Agent	Expan-	GPT-5 (high reasoning)	Create detailed, dataset-aware coding assessments that operationalize each hypothesis for validation.	Best available model; precise analytical instructions are critical for effective validation.
Coding Results Interpreter	Coding Instructions Agent, Hypothesis Expansion Agent, Coding Agent	GPT-5 (high reasoning + visual tools)		Analyze coding results, interpret statistical significance, and assess validation outcomes, assigning a feasibility score.	High-reasoning multimodal model; interpretation requires quantitative and visual analysis.
Summary Agent	Coding Results Interpreter, Hypothesis Expansion Agent, Novelty Critic Agent	Results	GPT-5 Mini	Generate a clear, concise summary presenting the final hypothesis, rationale, novelty score, and feasibility score.	Balanced model; synthesis task prioritizing clarity and structured reporting.

B.3. Feasibility Agent

Check table 6 for more details on the protocol of computing the feasibility score.

Table 6. Feasibility Agent evaluation protocol and scoring criteria.

Step	Weight	Description
Data Reality Check	35%	Verifies existence of suitable datasets, sample sizes, and required variables for hypothesis testing.
Tech-Stack Alignment	25%	Assesses maturity, availability, and maintenance status of analysis tools and reference implementations.
Logical Stress Test	25%	Identifies gaps in causal reasoning, confounders, and falsifiability of the proposed hypothesis.
Resource Constraints	15%	Evaluates computational requirements, runtime feasibility, and expected timeline.

Table 7. External tools used by the Feasibility Agent for evidence grounding.

Category	Tool	Purpose
Literature	PubMed	Biomedical literature search and validation
Literature	Semantic Scholar	Retrieval of peer-reviewed publications and citations
Datasets	GEO	Public gene expression datasets
Datasets	TCGA/GDC	Cancer genomics and clinical data
Clinical Trials	ClinicalTrials.gov	Identification of relevant clinical trials
Technical	PyPI	Verification of package availability and maturity
Technical	GitHub	Repository activity and maintenance status
Methods	Papers With Code	Identification of reference implementations

B.4. Tool Orchestration Subsystem

The tool orchestration subsystem is implemented as an MCP-based client–server architecture (Anthropic, 2024) that provides a unified control plane for interacting with heterogeneous clinical and computational tools, see figure 5. Acting as an intermediary between the coding agent/researcher and multiple domain-specific suites, the MCP Orchestrator interprets user prompts, analyzes task intent, dynamically selects the appropriate tools, and coordinates their execution. It enables seamless integration of medical oncology workflows (e.g., survival analysis and treatment selection) with histopathology pipelines (e.g., tumor, mitosis, tubule, TLS, and collagen segmentation, MIL, and foundation models), operating over shared patient-level data and whole-slide images. By abstracting tool location, implementation details, and execution logic, the subsystem supports scalable, modular, and extensible tool usage across distributed systems while maintaining a coherent prompt-to-result interaction model for hypothesis generation and downstream analysis. Figures 6 and 7 provide an illustrative example of how the tool orchestration subsystem can be accessed by a user or an autonomous agent through the system interface. In this example workflow, a histopathology whole slide image is uploaded and a tumor detection request is issued. The subsystem invokes the appropriate tumor segmentation tool and returns a binary tumor mask, followed by region-aware patch extraction in which tumor, peritumoral, and remaining tissue regions are overlaid on the image. These figures are intended to demonstrate the user-facing interface and the composition of detection and spatial reasoning tools, rather than to present quantitative performance results.

B.5. Validated End-to-End Example

Table 8 presents a representative validated hypothesis generated by SAGE, illustrating the full reasoning–validation pipeline from user prompt to feasibility assessment.

C. Rationale for Per-Agent Context in the Specific-Memory Architecture

Each agent in the *Specific-Memory Architecture* (*Graph-based pipeline (GP)*) receives a customized context containing only the information necessary for its specific task. This design prevents redundancy, reduces token consumption, and maintains each agent’s focus on relevant inputs. By contrast, the *Shared-Memory Architecture* (*Chat-based pipeline (CP)*) exposes every agent to the full conversation history, which increases cost and introduces unnecessary contextual noise. Check table 9 for more details.

Motivations for Context Design

Information is excluded from an agent’s context when it has already been integrated into the output of its predecessors. This ensures:

- Minimal token usage and predictable computational scaling.
- Avoidance of irrelevant or redundant information that could distract from the agent’s core reasoning task.
- Reduced risk of “context dilution,” where long prompts degrade LLM focus and increase hallucination.

D. Multi-Critic Novelty Evaluation

D.1. Evaluation Dataset and Protocol

We constructed a ground-truth dataset of 150 scientific proposals spanning five levels of novelty using time-travel backtesting to mitigate temporal leakage. Proposals were evaluated only against literature available prior to their publication or retraction. Table 10 summarizes the category definitions, ground-truth score ranges, and temporal evaluation windows.

Category composition. The five novelty categories span a continuum from transformative scientific advances to demonstrably invalid claims. Category A (*Breakthrough*) includes Nobel-winning discoveries and paradigm-shifting methods (e.g., AlphaFold2, CRISPR–Cas9) as well as foundational machine learning architectures (Transformer, ResNet, GAN). Category B (*High Novelty*) consists of significant advances that substantially extend prior work (e.g., GAT, BERT, ViT, SAM). Category C (*Moderate*) captures meaningful but non-paradigmatic contributions, such as novel combinations of existing techniques (e.g., multi-task learning, domain adaptation). Category D (*Incremental*) includes standard applications and routine extensions (e.g., YOLO variants, conventional SVM pipelines). Category E (*Specious*) comprises fabricated or invalid claims, including known frauds (STAP Cells), methodological failures (Arsenic Life), and measurement errors (ICEP2).

D.2. Deliberation Dynamics and Literature Retrieval

Table 11 reports how frequently deliberation is triggered across novelty categories, along with associated debate depth and literature retrieval behavior. These statistics characterize when deliberation activates and how critics gather evidence under disagreement.

As shown in Table 11, deliberation is triggered most frequently for extreme categories (A and E), where initial critic disagreement is highest. Breakthrough proposals retrieve fewer references with minimal contradiction, consistent with genuine gaps in prior literature, whereas specious claims exhibit high contradiction rates, validating the system’s ability to distinguish absence of evidence from evidence of contradiction.

D.3. Cross-Domain Validation

To assess generalizability, we evaluated the Multi-Critic system on 30 SAGE-generated biomedical hypotheses spanning multiple novelty categories. Model assessments demonstrated strong agreement with expert scores, achieving a Pearson correlation of $r = 0.91$ and a Spearman rank correlation of $\rho = 0.89$, indicating consistency in both absolute scoring and relative ranking. The mean absolute error was low ($MAE = 0.31$), suggesting tight alignment with expert judgments. Bias analysis revealed a slight conservative tendency for breakthrough hypotheses (mean signed error = -0.17), while moderately novel hypotheses exhibited a small positive bias ($+0.12$), reflecting mild overestimation in borderline cases.

D.4. Error Analysis

Across the evaluation set, we observed 13 misclassifications, corresponding to an overall error rate of 8.7%. The majority of errors arose from boundary ambiguity between creative application and incremental extension, accounting for 10 of the 13 cases. These typically involved hypotheses that combined established methods in novel contexts, where expert assessments varied in emphasis between originality and methodological extension. Two errors reflected underestimation of paradigm-shifting contributions, in which the system assigned high but not maximal novelty scores. A single failure case involved a historically specious claim that lacked explicit refutation in early literature snapshots, highlighting limitations inherent to temporally constrained evidence. Overall, errors were concentrated near category boundaries rather than gross misjudgments of novelty.

E. Example Generated Hypotheses

E.1. Original Hypothesis

In male TCGA-BLCA patients, high tumor ADRM1 expression combined with image-based immune exclusion—low (Tumor Infiltrating Lymphocytes) TIL density, low TIL margin enrichment, and paucity of TLS-like aggregates—predicts significantly worse overall survival than ADRM1-low or immune-infiltrated counterparts.

E.2. Refined Hypothesis

Among male TCGA-BLCA patients, high ADRM1 expression coupled with a stroma-rich histology (high stromal-to-tumor ratio) and low TIL margin enrichment on H&E images predicts inferior overall survival and progression-free interval, particularly when ECM/matriosome transcripts (e.g., FN1, COL1A1, COL3A1) and T-cell exhaustion signatures are upregulated. This ADRM1–stroma–immune imaging–genomic axis will show stronger adverse prognostic impact in patients with comorbid diabetes, consistent with diabetes-associated microenvironmental remodeling.

Compared to the Scientist Agent’s initial formulation, this refined hypothesis integrates stromal morphology, transcriptomic correlates, immune exhaustion signatures, and clinical comorbidities, illustrating how iterative refinement enhances biological coherence and clinical interpretability.

E.3. Prompt Refinement And Domain Adaptation Examples

This example illustrates the role of negative prompting in constraining unsupported quantitative speculation. The unrefined prompt produces precise hazard ratios and response-rate reductions without evidentiary grounding, reflecting a common hallucination mode of LLMs when numerical specificity is not explicitly discouraged. By contrast, the refined prompt intentionally challenges the model to avoid unverifiable effect sizes and mechanistic overreach, resulting in a qualitatively sound, testable hypothesis that preserves biological plausibility while deferring quantitative claims to downstream empirical validation. This demonstrates how negative prompting improves hypothesis fidelity by prioritizing evidence-consistent abstraction over spurious numerical precision.

Original prompt output (unrefined).

In radiotherapy-exposed male patients developing secondary primary bladder cancer, high ADRM1 expression (upper quartile RNA-seq RSEM ≥ 2.5 log₂ units) will be associated with a 1.8–2.2 \times increase in hazard ratio for overall survival and a 35–40% reduction in cisplatin-based chemotherapy response rate compared to ADRM1-low males. Mechanistically, ADRM1 overexpression may accelerate proteasomal degradation of DNA repair intermediates (e.g., ubiquitinated FANCD2, γ H2AX), leading to accumulation of unrepaired DSBs and clonal selection of chemoresistant tumor subpopulations.

Refined prompt output (negative prompting).

Among male patients who develop secondary primary bladder cancer following prior pelvic radiotherapy, high ADRM1 expression predicts poorer chemotherapy response and reduced overall survival, suggesting ADRM1 as a sex-specific biomarker of radiotherapy-related bladder cancer aggressiveness.

E.4. Examples under Memory-Constrained Inference

In male TCGA-BLCA patients, high tumor ADRM1 expression combined with image-based immune exclusion—low TIL density, low TIL margin enrichment, and paucity of TLS-like aggregates—predicts significantly worse overall survival than ADRM1-low or immune-infiltrated counterparts. This ADRM1–immune–spatial interaction remains prognostic after adjusting for stage and WSI-predicted basal/luminal subtype.

This hypothesis achieved a novelty score of 7/10 while reducing total token usage by approximately 65% compared to the shared-memory pipeline, illustrating that concise, domain-grounded reasoning can be preserved under context-constrained settings.

E.5. Example: High-Novelty, High-Feasibility Hypothesis Validation

Hypothesis generation and assessment. SAGE generated the following hypothesis, which was assigned a high novelty score (> 7) and high feasibility by the multi-critic evaluation module:

In TCGA-BLCA, high E-FABP (FABP5) expression combined with scarce TLS-like lymphoid aggregates on whole-slide images identifies patients with higher lymph-node positivity and significantly worse overall survival, whereas low FABP5 expression with abundant TLS-like aggregates marks a favorable-prognosis group.

This hypothesis integrates a molecular biomarker (FABP5 expression) with an imaging-derived immune spatial phenotype (TLS-like lymphoid aggregates), forming a multi-modal prognostic interaction that is not explicitly encoded in existing bladder cancer risk stratification frameworks.

Translation to an executable validation contract. The hypothesis was passed to the *Coding Instructions Agent (Planner)*, which translated the natural-language statement into an executable analysis specification. The resulting validation contract included:

- **Dataset:** TCGA-BLCA
- **Molecular variable:** FABP5 (E-FABP) RNA expression
- **Imaging-derived variable:** TLS-like lymphoid aggregate density on whole-slide images
- **Patient stratification:** Joint stratification by FABP5 expression (high vs. low) and TLS abundance (scarce vs. abundant)
- **Clinical endpoints:** Overall survival and lymph-node positivity
- **Statistical analyses:** Kaplan–Meier survival analysis, log-rank testing, and Cox proportional hazards modeling

This step converts a free-form hypothesis into a validation-centric contract, ensuring explicit alignment between the scientific claim and downstream analyses.

Agentic execution and validation. The executable specification was then handled by the *Coding Agent*, which acts as a controller coordinating specialized sub-agents. A *Task Agent* managed control flow and invoked a *Data Agent* to retrieve and align TCGA-BLCA molecular, clinical, and imaging-derived variables at the patient level. A *Validation Agent* subsequently performed survival analyses, including Kaplan–Meier curve generation, log-rank testing, and Cox proportional hazards modeling with confidence intervals. See figure 3.

Validation results. Kaplan–Meier survival analysis (Fig. 3) demonstrated clear separation between patient groups defined by the joint FABP5–TLS stratification. Patients with high FABP5 expression and scarce TLS-like aggregates exhibited significantly worse overall survival compared to those with low FABP5 expression and abundant TLS-like aggregates, with statistical significance confirmed by log-rank testing. Cox proportional hazards models further supported this association, indicating elevated risk in the high-FABP5 / low-TLS group.

Interpretation. The *Coding Results Interpreter* synthesized the statistical outputs and visualizations and concluded that the hypothesis is supported by the TCGA-BLCA data. This example demonstrates how SAGE generates hypotheses that are simultaneously high in novelty and feasibility.

MCP-Based Client-Server Architecture

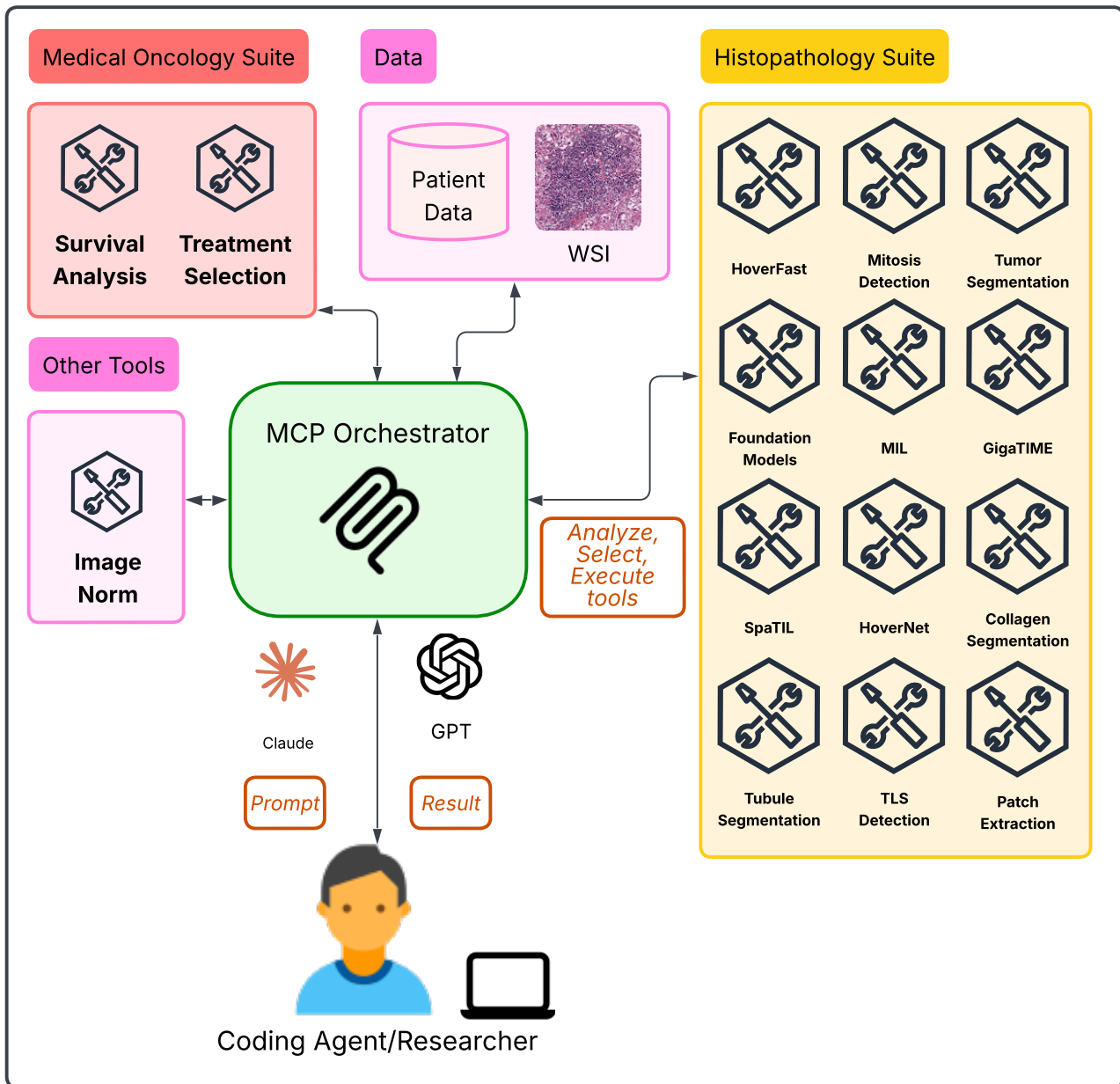


Figure 5. Overview of the Tool Orchestration Subsystem. MCP-based tool orchestration subsystem enabling unified access to clinical and computational tools across oncology and histopathology suites. The MCP Orchestrator mediates between a coding agent/researcher and distributed client-server tools by analyzing prompts, selecting appropriate capabilities, and executing them over shared patient data and whole-slide images.

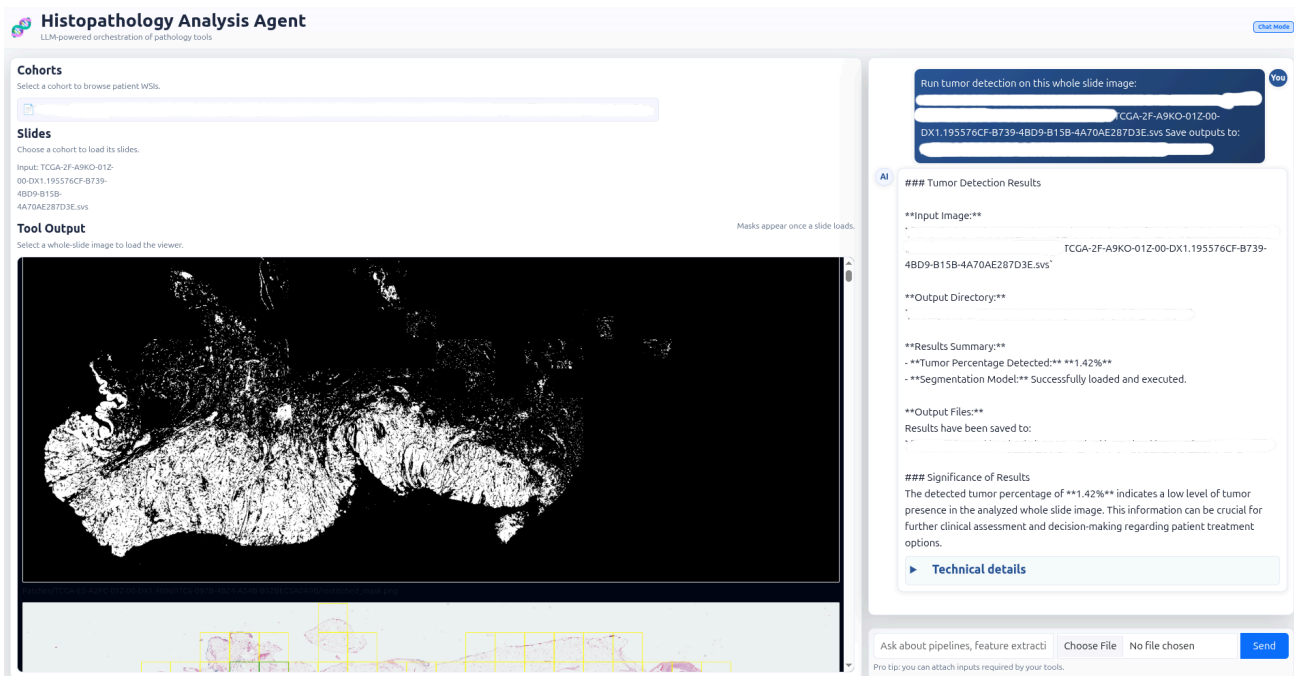


Figure 6. Tool orchestration subsystem for tumor detection on whole slide images. User interface of the tool orchestration subsystem responding to a tumor detection request on an input whole slide image. The system invokes the tumor segmentation tool and returns a binary tumor mask, highlighting detected tumor regions while suppressing non-tumor tissue.

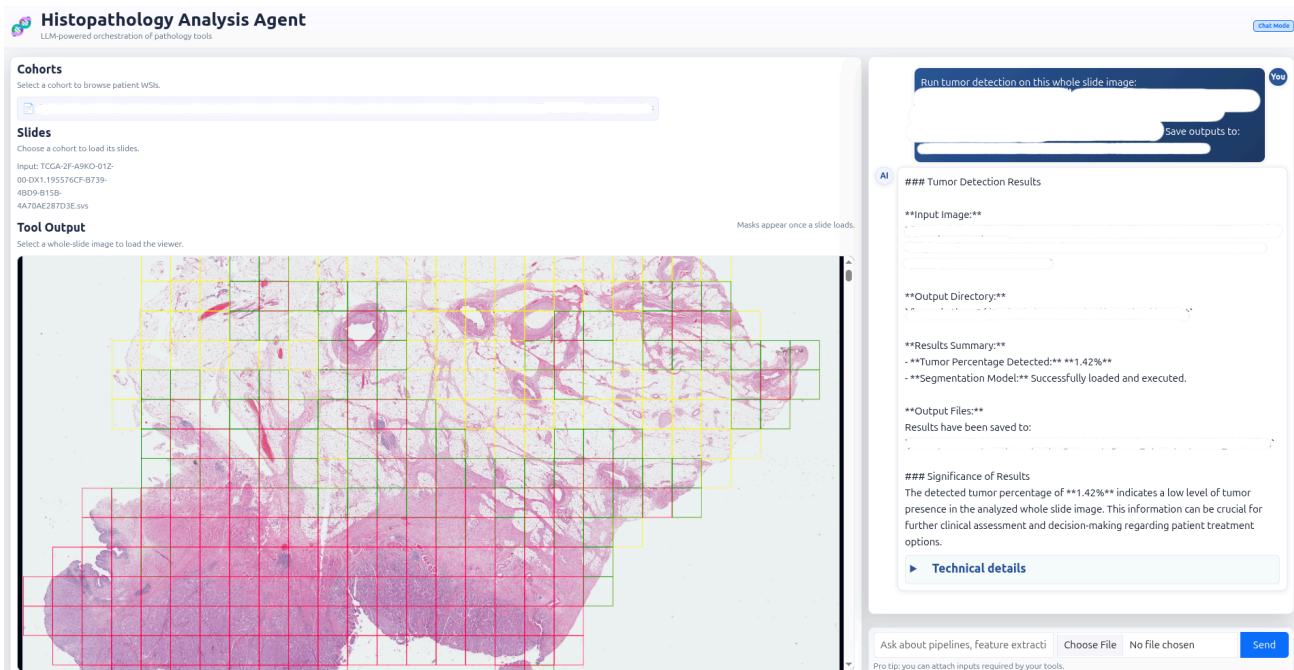


Figure 7. Region-aware patch extraction via tool orchestration. Visualization of region-aware patch extraction following tumor segmentation. The whole slide image is overlaid with color-coded patches corresponding to tumor regions (red), peritumoral regions (green), and remaining tissue (yellow). This figure illustrates how the tool orchestration subsystem composes segmentation, spatial reasoning, and patch extraction tools to generate structured outputs for downstream analysis.

Table 8. Validated SAGE-generated hypothesis for CXCL13 in muscle-invasive bladder cancer (MIBC). This table summarizes the full reasoning-validation workflow, from prompt to feasibility assessment.

User Prompt	Explore research ideas between <i>genetic-clinical based prognostic signature</i> and <i>locally advanced bladder cancer</i> .
Hypothesis	High CXCL13 expression increases immune activity-proxy sensitivity and improves progression-free interval in muscle-invasive bladder cancer.
Rationale	CXCL13 mediates B cell and T follicular helper (Tfh) recruitment and promotes tertiary lymphoid structure (TLS) formation. These immune niches enhance antigen presentation and CD8 ⁺ T-cell activation, contributing to improved clinical outcomes and immune checkpoint blockade (ICB) response in MIBC.
Novelty	Links CXCL13 to spatially organized immune architecture and TLS maturity—dimensions absent in existing MIBC biomarkers. Integrates transcriptomic, spatial, and clinical data to test mechanistic immune hypotheses rather than correlation alone.
Novelty Score	4 / 10
References	<ul style="list-style-type: none"> • Tertiary Lymphoid Structures are Linked to Enhanced Antitumor Immunity and Better Prognosis in MIBC (Link) • Abstract 1195: BC-BET v2.0—Updates to an Online Bladder Cancer Biomarker Evaluation Tool (Link)
Coding Tasks	<ul style="list-style-type: none"> • Immune activation proxy association with CXCL13 expression (dataset: TCGA_BLCA_firehose_legacy) • Spatial immune cell co-localization and TLS maturity analysis (dataset: SpatialTranscriptomics_TCGA_Bladder)
Feasibility	The hypothesis is supported by consistent and statistically significant survival benefits for CXCL13-high patients across both univariate and multivariable analyses (HR ≈ 0.62 for PFS, HR ≈ 0.64 for OS, $p < 0.01$). These effects remain after adjusting for key covariates, indicating robustness within the dataset. However, the “immune activity-proxy sensitivity” component has not been directly evaluated, and further immune profiling and external validation are required to confirm mechanistic links and clinical translatability.
Feasibility Score	8 / 10

Table 9. Context allocation per agent in the Specific-Memory Architecture (GP). Each agent receives only the information essential to its function, avoiding redundant or indirectly relevant data.

Agent	Context Provided	Context Excluded	Rationale
<i>Path Generation Agent</i>	Initial user query in natural language	N/A (pipeline start)	Needs only the query to generate knowledge-graph paths.
<i>Ontologist</i>	All paths generated by the Path Generation Agent	Initial user query	Paths already encode query intent; user query would be redundant.
<i>Scientist</i>	Definitions and relationships from Ontologist	Paths from Path Generation Agent	Ontologist output already refines path information.
<i>Hypothesis Expansion Agent</i>	Concise hypothesis from Scientist	Ontologist and Path Generation outputs	Scientist hypothesis synthesizes upstream information; earlier outputs add noise.
<i>Novelty Critic Agent</i>	Expanded hypothesis and justification from Hypothesis Expansion Agent	All previous outputs (Scientist, Ontologist, Path Generation)	Needs only the final hypothesis for literature-based comparison.
<i>Coding Instructions Agent</i>	Expanded hypothesis and justification from Hypothesis Expansion Agent	All previous conceptual outputs (Scientist, Ontologist, Path Generation)	Uses hypothesis details to design validation assessments.
<i>Coding Results Interpreter</i>	Expanded hypothesis, coding instructions, and results	Upstream conceptual outputs (Ontologist, Path Generation)	Requires hypothesis, instructions, and results for statistical interpretation.
<i>Summary Agent</i>	Coding Results Interpreter, Hypothesis Expansion Agent, and Novelty Critic Agent	Coding Instructions, Ontologist, and Path Generation Agents	Needs validation results, final hypothesis, and novelty score for synthesis.

Table 10. Evaluation dataset composition and temporal evaluation protocol.

Category	n	Ground Truth	Evaluation Time
A: Breakthrough	30	8.5–10.0	2 years pre-publication
B: High Novelty	30	7.0–8.5	1 year pre-publication
C: Moderate	30	5.0–7.0	Publication year
D: Incremental	30	3.5–5.0	Publication year
E: Specious	30	1.0–3.5	Post-retraction
Total	150	—	—

Table 11. Debate frequency and literature retrieval statistics across novelty categories.

Category	Debate Triggered	Rounds (Avg.)	Refs Retrieved	Contradictions Found
A: Breakthrough	76.7%	2.43	4.4 ± 1.8	0.3 ± 0.6
B: High Novelty	63.3%	2.11	5.9 ± 2.2	1.2 ± 1.1
C: Moderate	46.7%	1.64	8.0 ± 2.8	3.8 ± 1.8
D: Incremental	40.0%	1.50	9.4 ± 3.1	6.2 ± 2.3
E: Specious	83.3%	2.68	8.5 ± 3.2	8.7 ± 2.9